

Effect of Grain Size on Flexoelectricity

Zhiguo Wang,^{1,†} Chunchun Li^{2,†} Hongyuan Xie,^{1,‡} Zhen Zhang,¹ Wenbin Huang,³ Shanming Ke,¹ and Longlong Shu^{1,*}

¹*School of Materials Science and Engineering, Nanchang University, Nanchang 330031, People's Republic of China*

²*College of Materials Science and Engineering, Guilin University of Technology, Guilin 541004, People's Republic of China*

³*The State Key Lab of Mechanical Transmissions, Chongqing University, Chongqing 400044, People's Republic of China*



(Received 22 March 2022; revised 2 September 2022; accepted 22 September 2022; published 7 December 2022)

The grain-size effect of permittivity has been widely studied and its phenomenological theory is well established. In this work, we use such grain-size-effect theory to examine the grain-size effect of flexoelectricity, which has been overlooked so far. Two typical flexoelectric materials are employed, namely, ferroelectric BaTiO₃ ceramics and paraelectric SrTiO₃ ceramics. The results suggest that the variation of the intrinsic flexoelectric coefficient is completely synchronized with the variation of the grain-size-dependent permittivity for SrTiO₃ ceramics. However, this synchronization is overturned in BaTiO₃ ceramics, the flexoelectric coefficient of which increases with the grain size rather than dielectric permittivity. Under a flexoelectric field, it is proven that the polarization deflection of the 180° domains (more likely to exist for large grain sizes) dominates the flexoelectricity of ferroelectric BaTiO₃ ceramics. The observed flexoelectric grain-size effect is beneficial for the design of bulk materials with a high flexoelectric coefficient and provides a simple and effective way to improve the performance of actuators and sensors based on bulk flexoelectricity.

DOI: 10.1103/PhysRevApplied.18.064017

I. INTRODUCTION

The flexoelectric effect, similar to the well-known piezoelectric effect, is an electromechanical coupling of polarization induced by a strain gradient [1–6]. Contrary to piezoelectricity, flexoelectricity can exist in a variety of materials, including solid dielectrics [7,8], liquid crystals [9,10], and semiconductors [11,12], regardless of the crystallographic symmetry, since the flexoelectric coefficient, μ_{ijkl} , is a fourth-rank tensor. The promising potential of replacing piezoelectricity with flexoelectricity has been highlighted [13,14], such as in energy harvesting [15] and equivalent piezoelectric devices based on the bulk flexoelectric effect [16]. The flexoelectric coefficient directly reflects the electromechanical coupling ability and the high-value μ_{ijkl} renders the excellent performance of flexoelectric dielectric devices [17–19]. Theoretical studies establish the direct correlation between the flexoelectric coefficient and the dielectric permittivity [20–24]. In addition, through a change in the temperature environment, the positive correlation between the flexoelectric coefficient and the dielectric permittivity is experimentally

obtained [25–27]. Therefore, it is feasible to develop high flexoelectric activity in materials with a high dielectric constant.

At present, there are many methods to improve the dielectric permittivity of materials, including defect engineering [28,29] and domain engineering [30,31]. Alternatively, the dielectric permittivity can be directly regulated by controlling the grain size of ceramics without changing the macroscopic structure [32–34]. In polycrystalline ferroelectrics, grain size plays an important role in the physical properties, including the dielectric permittivity, piezoelectric coefficient, and spontaneous polarization. Typically, the effects of grain size on the electrical properties of ferroelectric ceramics (such as barium titanate BaTiO₃, hereinafter referred to as BTO) have been intensively explored [35–38]. It is widely accepted that, with an increase of the grain size to a characteristic value (around 1 μm in BTO), the relative dielectric permittivity and piezoelectric coefficient reach their relative maximum values [39–41]. This grain-size effect originates from both intrinsic and extrinsic factors. The intrinsic contribution generally refers to the lattice and its deformation [42–44], while extrinsic factors are related to the enhanced motion of 90° domain walls in the defect environment [38,45].

*llshu@ncu.edu.cn

†Z. Wang, C. Li, and H. Xie contributed equally to this work.

In consideration of the mutual correlations of the grain size versus the dielectric permittivity, and the dielectric permittivity versus the flexoelectric coefficient, it is of great significance to study the grain-size effect on flexoelectricity to improve the flexoelectric coefficient of materials. Here, the relationship between the grain size and flexoelectricity in BTO is established. In addition, the typical paraelectric material SrTiO₃ (STO) is investigated to exclude the effect of ferroelectricity. This work extends the grain-size effects to the physical context and sheds light on the improvement and adjustment of flexoelectricity via microstructure engineering.

II. EXPERIMENTAL DETAILS

BTO ceramics are prepared by solid-phase sintering of nanosized BaTiO₃ (99.8%, Aladdin) powders as the raw materials. These powders are granulated with polyvinyl alcohol solution and pressed into shape at a pressure of 20 MPa. Finally, the eight series of BTO ceramics are sintered at 1150–1400 °C for 6–10 h. The same method is used for the preparation of STO ceramics, which are sintered at 1250–1600 °C. Next, after the samples are sintered, annealing is undertaken again through a tube furnace at 800 °C for 10 h in an air atmosphere. The purpose of this is to eliminate oxygen vacancies caused by sintering.

The phase composition is characterized by x-ray diffraction (XRD) using a D/Max-IIIC x-ray diffractometer (Rigaku, Tokyo, Japan) with Cu K α radiation. The Raman spectra are recorded by using a confocal Raman spectrometer (WITec, Alpha 300R, Germany). The microstructures of the natural surfaces and acid-etched surfaces are observed by using a scanning electron microscopy (SEM, Model JSM 6710F, Jeol, Japan). The samples are polished and coated with a gold electrode on both sides for subsequent dielectric characterization. The dielectric properties of the ceramics are measured by using a broadband

dielectric spectrometer (Concept 40, Germany) and an impedance analyzer (E4294A, Agilent, Palo Alto, USA). The ferroelectric hysteresis loops (P - E loops) are analyzed using a ferroelectric integrated test system (airACCT-2000E, Germany). The piezoelectric properties, d_{33} , are characterized by a quasistatic d_{33} instrument (ZJ4AN, China). The flexoelectric coefficients are measured through a dynamic thermomechanical analysis system (DMA, DMA 850, TA Instruments, USA). The thermally stimulated depolarization current (TSDC) of the ceramic pellets is measured using a pA meter (6517B, Keithley, Cleveland, OH) and a temperature controller (SPIV17T-843F, PK, USA) for temperature-dependence measurements.

III. RESULTS AND DISCUSSION

A. Structural changes with the grain sizes of BTO and STO ceramics

Direct evidence of the grain size at different sintering temperatures is provided by SEM. The SEM images of the natural surface for BTO ceramics are shown in Fig. 1, where dense microstructures, clear grain boundaries, and few visible pores are developed. An increase in temperature results in an increase in the relative density from 95.7% at 1150 °C to 98.4% at 1400 °C. With increasing temperature, the average grain size increases from 1.12 to 43.8 μ m, and the average grain size as a function of sintering temperature and time is listed in Table S1 (see Supplemental Material S1 [46]). A similar phenomenon is also observed in STO ceramics (see Supplemental Material S1 [46]). When the sintering temperature increases from 1250 to 1600 °C, the average grain size of the STO ceramics increases from 0.39 to 10.1 μ m.

The room-temperature XRD patterns of BTO ceramics fired over a temperature range of 1150–1400 °C are shown in Fig. 2(a). All the observed diffraction peaks belong to BTO and no other peaks of impurities are present. This

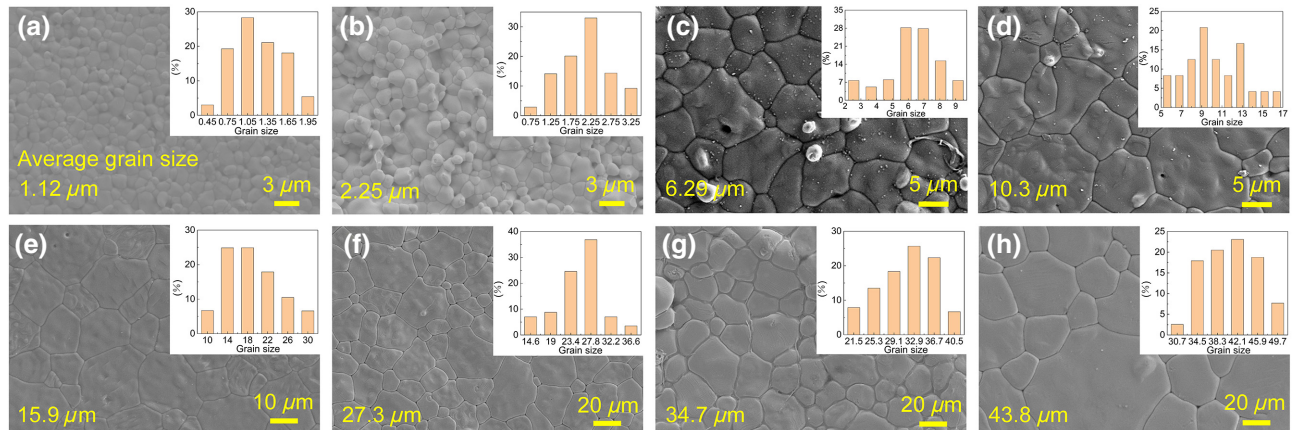


FIG. 1. SEM images of natural surfaces of BaTiO₃ ceramics with different grain sizes: (a) 1.12 μ m, (b) 2.25 μ m, (c) 6.29 μ m, (d) 10.3 μ m, (e) 15.9 μ m, (f) 27.3 μ m, (g) 34.7 μ m, (h) 43.8 μ m. Insets are size distributions of BaTiO₃ grains.

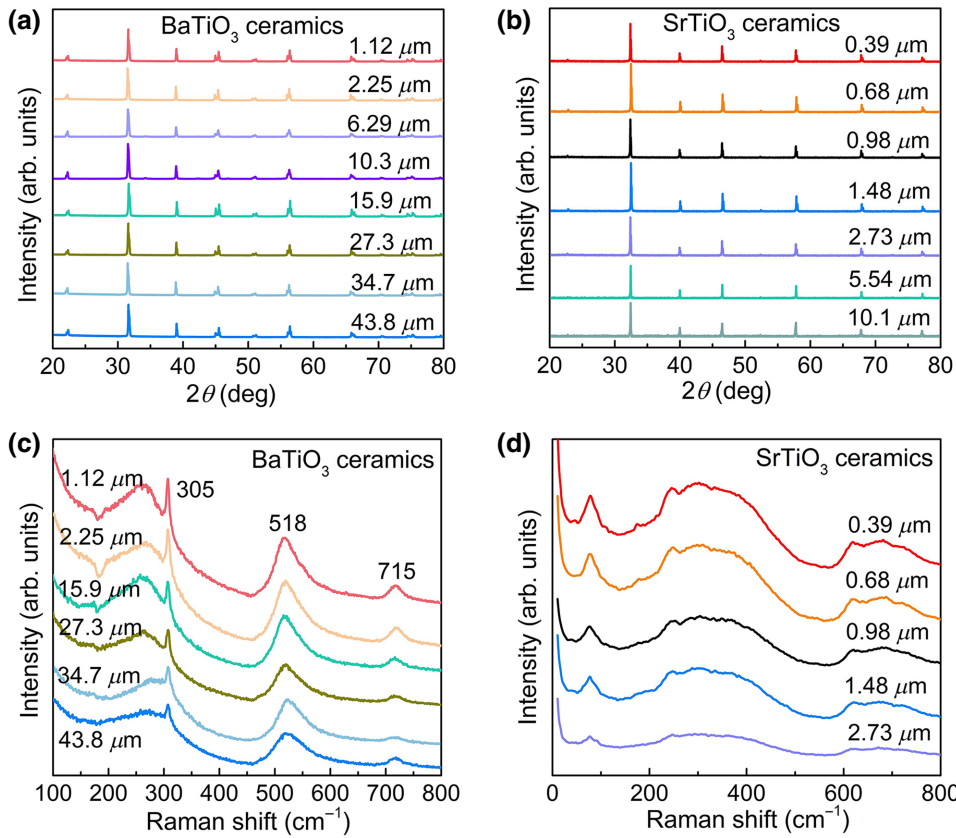


FIG. 2. XRD patterns of (a) BaTiO₃ and (b) SrTiO₃ ceramics. Raman spectra of (c) BaTiO₃ and (d) SrTiO₃ ceramics formed at different sintering temperatures.

result proves the formation of single-phase BTO and suggests that different sintering temperatures result in limited variation in the macrostructure of BTO. For STO ceramics, the phase constitution is determined by XRD and is shown in Fig. 2(b). All STO ceramics crystallize in a cubic perovskite structure with no second phase detected, which confirms the phase purity of the as-prepared ceramics. In addition, the effect of bulk density on the dielectric permittivity is significant [55,56], which will inevitably affect the flexoelectric coefficient. For BTO ceramics, the average grain size increases from 1.12 to 43.8 μm, and the relative density increases from 95.7% to 98.4%. Correspondingly, the fractional porosity drops from 4.3% to 1.6%. The corrected permittivity (ϵ_{corr}) is calculated with the aim of eliminating the influence of porosity on the permittivity using the Bosman and Having's equation, as follows [57]:

$$\epsilon_{\text{corr}} = \epsilon_r(1 + 1.5p), \quad (1)$$

where p is the fractional porosity and ϵ_{corr} is the corrected value. It can be seen that $1.5p$ is the difference between the corrected permittivity and the measured permittivity. This value will drop from 6.4% to 2.4% as the average grain size changes from 1.12 to 43.8 μm. Relative to the change in the flexoelectric coefficient (discussed in Sec. III D), from 2.5 μC/m for an average grain size of 1.12 μm to 25 μC/m for average grain size of 43.8 μm (10-fold

increments), the change in error between the corrected and measured permittivity is small. As a consequence, it is safe to conclude that the bulk density and the second phase of the ceramics are not the main factors of the flexoelectric grain-size effect.

Oxygen vacancies are easily generated in ceramics during sintering. If the concentration of oxygen vacancies is sufficient to significantly increase the conductivity of BTO and STO, the capacitor will behave like a Maxwell-Wagner system, where the response is dominated by the interfacial barrier layer. In this scenario, the dielectric and flexoelectric coefficients will be larger than the intrinsic (dielectric) values [11]. It appears that secondary annealing effectively removes defects, such as oxygen vacancies, which can be confirmed from the TSDC, as well as conductivity measurements (see Supplemental Material S2 [46]). In addition, the lattice constants obtained by XRD are close to the standard card values (see Supplemental Material S3 [46]), and the low dielectric loss (see Supplemental Material S4 [46]) also provides evidence for the lack of oxygen vacancies. Therefore, the influence of defects on flexoelectricity can be minimized by secondary annealing [53].

Although no changes are observed in the macrostructure, the microstructure changes demonstrated by Raman spectroscopy provide evidence of the grain-size effect. Figure 2(c) shows the Raman spectra for BTO samples

with various average grain sizes. Similar spectra with three main peaks located at 305, 518, and 715 cm⁻¹ can be observed, irrespective of the average grain sizes, which also confirms that no phase transition occurred over the entire sintering temperature. The sharp fingerprint Raman mode at 305 cm⁻¹, corresponding to the stretching vibration of the Ti—O bond, provides evidence of the tetragonal structure. With increasing sintering temperature (increasing grain size), the Raman intensity of the peak at 305 cm⁻¹ increases, which reflects the enhanced tetragonal characteristics [58,59]. Similarly, the Raman spectra of STO ceramics are shown in Fig. 2(d). As the sintering temperature increases, the average grain size increases, and the position of the main peaks does not change in any of the samples, indicating that no phase transition occurs.

B. Grain-size effect of permittivity and piezoelectricity

The variation of dielectric permittivity with grain size also provides evidence of the grain-size effect. Figure S4(a) within the Supplemental Material [46] shows the dielectric permittivity and loss of BTO ceramics sintered at different temperatures. A sharp peak is observed in the dielectric permittivity around $T_c \sim 120\text{--}130^\circ\text{C}$ for all samples, which corresponds to the phase transition from the paraelectric to ferroelectric phase [60]. All BTO samples show low dielectric losses on the order of 0.03. The dielectric permittivity at room temperature and T_c are listed in Fig. 3(a), where all ε_{\max} values at T_c are in the range of 11 000–12 000. Obviously, the dielectric permittivity of samples with grain sizes of 1.12 and 2.25 μm exhibit relatively high values at room temperature, while the samples with a grain size over 10 μm have a more significant decrease. In general, the dielectric permittivity shows a steadily decreasing trend as the sintering temperature increases, which is consistent with results in the literature [61]. This relationship is more complex for the dielectric permittivity of STO ceramics. As shown in Fig. S4(b) in the Supplemental Material [46], the dielectric permittivity behaves analogously for all samples, exhibiting a continuous decline along with increasing temperature, which is in accordance with the paraelectric state of STO. From the dielectric permittivity at room temperature [Fig. 3(b)], we can see that the dielectric permittivity increases first and then decreases with an increase of the average grain size. When the grain size is about 1 μm , the dielectric permittivity reaches the maximum value (~ 230). Although the trends are different for BTO and STO ceramics, the dependence of the dielectric permittivity on the grain size confirms the influence of the grain-size effect.

The ferroelectricity and piezoelectricity of ferroelectric BTO ceramics as a function of grain size provide further evidence of the grain-size effect. Ferroelectricity and residual piezoelectricity are considered to be important causes of high flexoelectricity for ferroelectric materials [7],

which have a direct enhancing effect on the flexoelectric coefficient. Therefore, the grain-size effect of the ferroelectricity of BTO ceramics is characterized and analyzed. As shown in Fig. 3(c), all samples represent the shape of a typical ferroelectric hysteresis loop and have a low coercive field. It can be confirmed that, with an increase in the sintering temperature, the coercive field hardly changes, but the saturated polarization intensity decreases slightly. In addition, the secondary annealing process can result in residual stress and macroscopic piezoelectricity being absent in the sample. Furthermore, for the cantilever-beam measurement configuration, the upper and lower parts of the sample endure the strain of the opposite sign. Hence, even if there is a remnant piezoelectric effect, the net effect in the entire sample should be zero, since the piezoelectric polarization created in the upper and lower halves cancels out [26,62]. In conclusion, although the residual piezoelectricity cannot be characterized, flexoelectric measurements can help us to exclude its influence, so as to ensure that the obtained signal originates from flexoelectricity.

Figure 3(d) shows the piezoelectric coefficient, d_{33} , after polarization of all BTO ceramic samples, which exhibits a gradually decreasing trend with an increase in the sintering temperature. The extreme d_{33} value of 386 pC/N appears in the BTO sample with a grain size of 1.12 μm . Then, d_{33} values of the subsequent samples are 334, 296, 249, 227, 184, 179, and 160 pC/N, respectively. This shows that the piezoelectricity of BTO ceramics is closely dependent on the grain size. At the same time, in the following, the piezoelectric grain-size effect is also helpful to understand the flexoelectric size effect of BTO ceramics induced by polarization deflection of domains.

C. Permittivity-induced flexoelectric grain-size effect on paraelectric STO ceramics

The cantilever-beam system is used to test the flexoelectric coefficient (see Supplemental Material S2 [46] for details). Figures S4(a) and S4(b) in the Supplemental Material [46] show the relationship between the bending-induced polarization and the strain gradient of BTO and STO samples with different grain sizes, respectively. The slope of the fitted dotted lines represents the flexoelectric coefficient. For paraelectric STO ceramics (ferroelectricity and residual piezoelectricity are excluded), the function of the flexoelectric coefficients, μ_{eff} , and grain sizes is shown in Fig. 4(a). When the grain size ranges from 0.39 to 10.1 μm , the flexoelectric coefficient increases first and then decreases with an increase in the grain size. The maximum flexoelectric coefficient (~ 13 nC/m) occurs when the grain size is 1 μm , which is consistent with the variation of the dielectric constant with grain size [Fig. 3(b)]. In addition, these flexoelectric coefficients are also of the same order of magnitude as those obtained in single crystals by Zubko *et al.* [14] and Mizzi *et al.* [63]. This result further

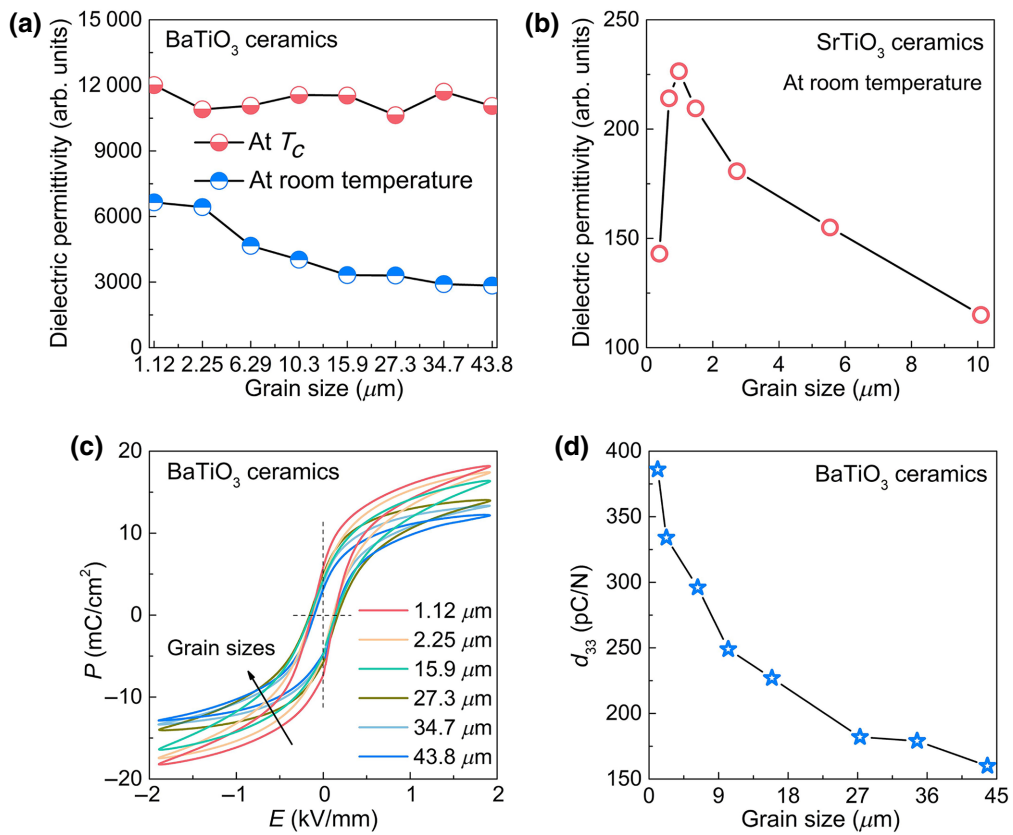


FIG. 3. (a) Dielectric permittivity of BaTiO_3 ceramics at T_c and room temperature. (b) Dielectric permittivity of SrTiO_3 ceramics at room temperature. (c) Hysteresis loop and (d) d_{33} of BaTiO_3 ceramics sintered at different temperatures.

confirms that, in the absence of external factors such as ferroelectricity, the flexoelectricity of materials is dielectric permittivity dependent [21–23].

Furthermore, to better analyze the dependence of flexoelectricity on the grain size, the effect of dielectric permittivity is excluded by normalization. For this purpose, the effective flexocoupling coefficient, γ , namely, the division of the effective flexoelectric coefficient by the dielectric permittivity, is employed [21]. In theory, for a linear dielectric, the intrinsic γ should be in the order of 1–10 V [62,64]. For STO ceramics, γ of all samples is less than 10 V [Fig. 4(b)], demonstrating the intrinsic flexoelectricity of the material. In addition, with an increase in grain size, γ changes from a rapid increase to a slow decrease and shows a maximum value at about 1 μm . The variation of the flexocoupling coefficient with grain size provides strong evidence for the intrinsic flexoelectric grain-size effect of STO ceramics.

D. Flexoelectricity for ferroelectric BTO ceramics

The dielectric permittivity dependency is broken in BTO ceramics. As shown in Fig. 4(c), when the grain size of BTO ceramics ranges from 1 to 45 μm , the flexoelectric coefficients increase from 2.5 to 25 $\mu\text{C/m}$. The

flexoelectric coefficients obtained in ceramics with an average grain size of 15–20 μm are consistent with those measured by Ma and Cross [65]. The flexoelectric coefficients are positively correlated with the grain sizes, which is opposite to the relationship between dielectric responses and grain sizes [Fig. 3(a)]. Furthermore, the relationship between the flexoelectric coefficient of BTO ceramics and temperature is characterized, and shown in Fig. S4(c) Supplemental Material [46]. The flexoelectric temperature spectrum increases, to a certain extent, while all the samples are close to the phase-transition temperature, which is consistent with the change of dielectric permittivity with temperature. In addition, smaller grains are consistently associated with smaller flexoelectric coefficients within the tested temperature range. The results preliminarily exclude the leading effect of dielectric permittivity on the flexoelectric grain-size effect of BTO ceramics.

Excluding the influence of the dielectric permittivity is necessary to find the extrinsic factors in determining the flexoelectric grain-size effect for BTO ceramics. For all samples [Fig. 4(d)], γ exceeds 10 V, indicating the enhancement of ferroelectricity to flexoelectricity [66]. Although the γ values are much higher than the intrinsic values (1–10 V) at room temperature, they present a steady growth with an increase in grain size, which is

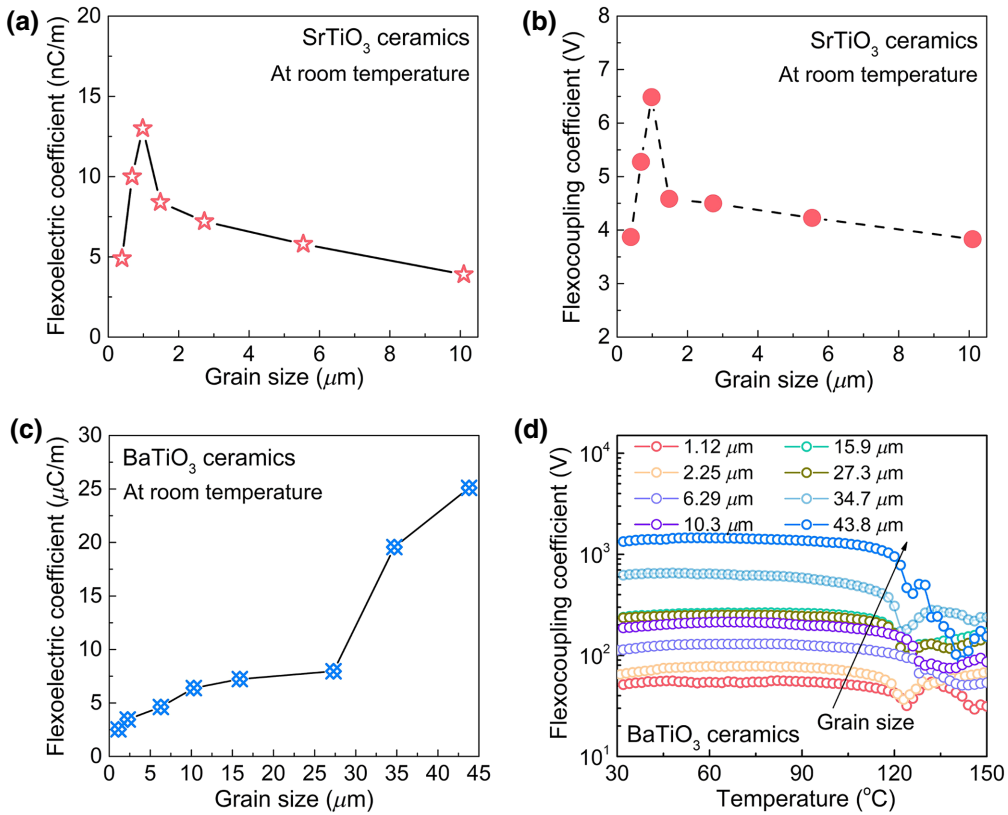


FIG. 4. Relationship between (a) flexoelectric coefficient and (b) flexocoupling coefficient γ and the grain size of SrTiO₃ ceramics. Relationship between (c) flexoelectric coefficient and grain size, and (d) flexocoupling coefficient γ and temperature of BaTiO₃ ceramics.

opposite to the grain-size effect of dielectric properties [Fig. 3(a)]. This result indicates that the dielectric coefficient contributes to the flexoelectricity, to some extent, but it does not play a leading role in the grain-size effect of nonintrinsic flexoelectricity. In addition, the flexoelectric and piezoelectric properties show opposite trends with the variation of grain size [Fig. 3(d)]; thus, the possibility that the residual piezoelectricity of BTO itself is a major contributor to the flexoelectricity grain-size effect can be ruled out. To explain the origin of the flexoelectric grain-size effect, we note that, with increasing grain size, 180° domains are more likely to occur within grains [67]. In contrast, the ceramic grains of small size tend to be dominated by 90° domains, thus increasing the limiting effect of grain boundaries. Therefore, another point is raised here about the underlying mechanism for the observed variation in flexoelectricity with the grain size.

E. Orientation of 180° domains under the flexoelectric field-induced flexoelectric grain-size effect for ferroelectric BTO ceramics

As shown in Figs. 5(a)–5(c), electric domain structures of polished BTO ceramics are observed. For samples with small grain sizes, the domains are mainly composed of

a series of parallel banded structures through the whole grains. This band structure is composed of 90° domains arranged alternately [68–70]. The 90° domains are created to relieve the large stresses that occur in BTO ceramics during the transition from the paraelectric phase to the ferroelectric phase with spontaneous polarization [71]. At the same time, with an increase in grain size and depolarization energy, watermark-shaped domains will appear in the grains, which are thought to consist of 180° domains [68,69,72].

In the spontaneously polarized domain region, polarization is the vector sum of the polarization dipoles, and it is directional. We can convert polarization into a combination of the polarization vectors along the thickness and horizontal directions. When bending the sample, the strain gradient is generated and induces a flexoelectric field in the thickness direction. Although this flexoelectric field is much weaker than the coercive electric field, the electric displacement in the thickness direction can still be produced, resulting in an increase or decrease of the polarization in the thickness direction. When the polarization vector in the thickness direction is combined with the polarization vector in the horizontal direction, it shows that the polarization intensity is driven by the flexoelectric field and “deflected” in the direction of this

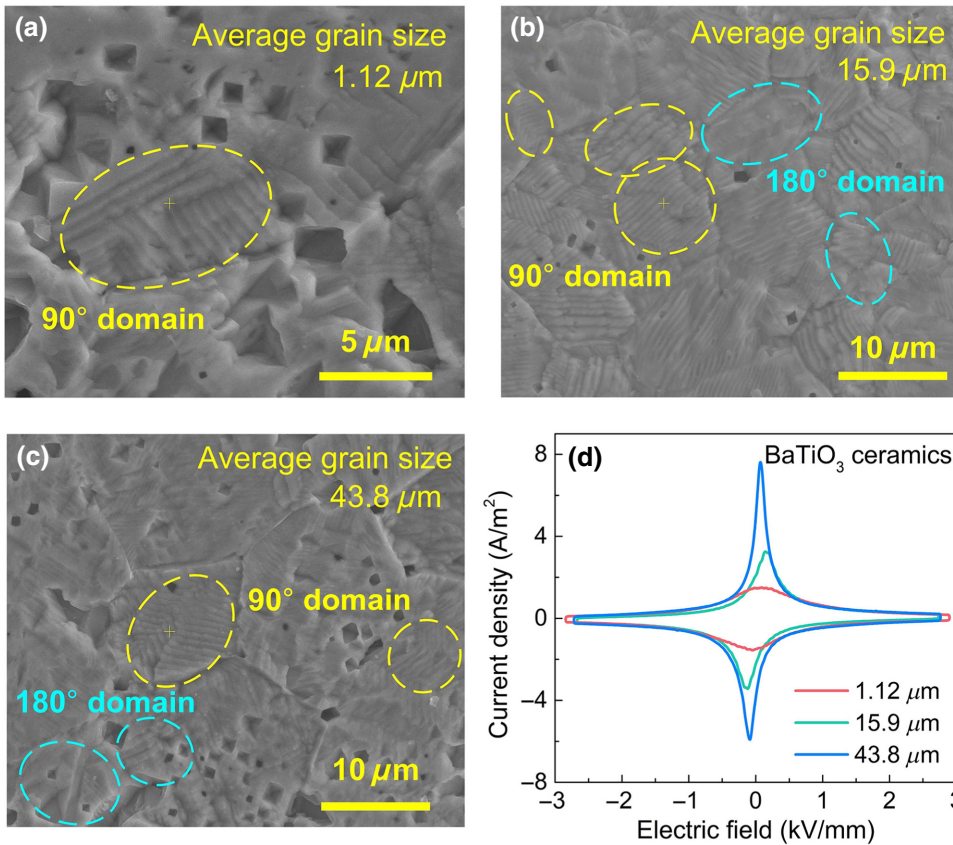


FIG. 5. Domain structure of BaTiO₃ ceramics sintered at (a) 1150 °C, (b) 1250 °C, and (c) 1350 °C. (d) Comparison of the I - E curves of BaTiO₃ ceramics at different sintering temperatures.

electric field. Among them, strong internal stress will be produced by the 90° domains in the ceramics, and due to the stress limitation at the grain boundary [73,74], polarization deflection of the 90° domains is more difficult than that of the 180° domains [72]. The latter is not restricted by adjacent grains because it does not cause changes in internal stress [75,76]. This effect of the flexoelectric field on different domains can be described by a simple model (Fig. 6). A flexoelectric field is generated when a strain gradient is applied to the sample through bending. When the flexoelectric field is applied to the 90° domains [Fig. 6(a)], polarization can be deflected only by small angles due to strong constraints from the grain boundary (shown by the thicker solid red lines). However, the grain boundary constraint is no longer present (shown by thinner solid red lines) for 180° domains; thus, it will become easier for the polarization of domains to be deflected with the field [Fig. 6(b)].

To further verify the effect of electric domains, the I - E curves of BTO ceramics with different grains are characterized [Fig. 5(d)]. Each curve has two current peaks corresponding to the polarization-current peak generated by the switching of the domains under the electric field, where the electric field corresponding to the current peak is the coercive field, E_c [77]. The current peaks generated by the switching of domains in the large-grain-size ceramics are more spiculate in shape, while the current peaks of the

small-grain-size samples are wider. The reason is that the proportion of the unstressed 180° domain increases as the grain size increases, and when the electric field exceeds the coercive field, the switch will be completed quickly over a narrow range of electric fields. In contrast, the switching of the 90° domains is a gradual process and will be accomplished over a wide range of electric fields. The results confirm the existence of more 180° domains in large-grain-size ceramics and the fact that 180° domains are more easily turned than 90° domains.

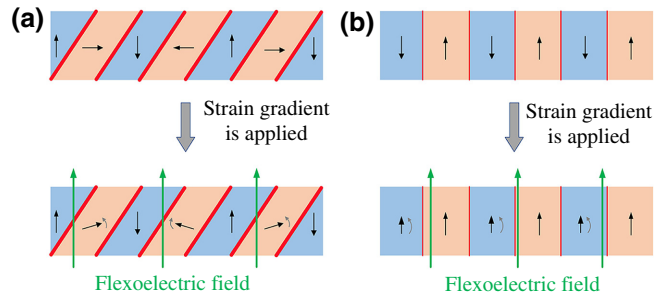


FIG. 6. Schematic diagram of the rotation of electric domains under the flexoelectric field. It is more difficult for (a) 90° domains to rotate with the flexoelectric field due to stronger grain boundary constraints (solid red line), relative to (b) 180° domains.

The macroscopic piezoelectricity of piezoelectric ceramics can be observed only after polarization, so the level of electric domain orientation after polarization determines the piezoelectric activity. As an index to measure the orientation of the electric domain, the residual polarization is very important to the piezoelectric size effect [78]. Therefore, a larger piezoelectric coefficient, d_{33} , is consistent with larger residual polarization in the smaller-grain-size BTO ceramics [Fig. 3(c)].

However, unlike piezoelectricity, the expression for flexoelectricity does not require polarization of the samples, which makes the ceramic domains exist in an initially disordered state. When bending the ceramics, assuming that the average strain gradient is in the order of $\partial\varepsilon_{11}/\partial x_3 \approx 0.01 \text{ m}^{-1}$, and the intrinsic γ is in the order of $f \approx 30\text{--}300 \text{ V}$ in the paraelectric phase (when $T > T_c$), the equivalent flexoelectric field of the ceramics is in the order of $E = f(\partial\varepsilon_{11}/\partial x_3) \approx 0.3 \sim 3 \text{ V/m}$, which is much smaller than the coercive field. The existence of polarization deflection can be confirmed by the change of the out-of-plane phase angle for the BTO ceramic's domain using piezoresponse force microscopy at different voltages (see Supplemental Material S7 [46]). Although such a flexoelectric field is weak, relative to the coercive electric field, it can still provide a driving force to deflect the polarization of domains toward the direction of the flexoelectric field [79]. Therefore, in contrast to the piezoelectric effect, BTO ceramics with a large grain size can induce more external bend-induced charges under a weak electric field (flexoelectric field) and exhibit higher flexoelectric coefficients, due to the presence of more-easily-polarization-deflected 180° domains.

It is worth noting that, in addition to the domain types (90° and 180° domains), the flexoelectric coefficient is still affected by a variety of other factors, including oxygen vacancies [53] and domain boundaries [54]. For this reason, the interference from oxygen vacancies on the flexoelectricity will be effectively excluded by secondary annealing. On the other hand, as the size of the ceramic grain increases, the domain size also increases and the domain-wall density decreases [80]. A higher domain-wall density is beneficial for reducing the free-energy barrier for domain flipping [54,81]. This also contradicts the relationship between flexoelectricity and grain size; therefore, we believe that the role of domain walls is not the main factor in inducing the flexoelectricity grain-size effect. Although they are not the main inducers of the flexoelectric grain-size effect, their contribution to the flexoelectric coefficient cannot be ignored.

IV. CONCLUSION

With grain sizes ranging from 0.39 to $10.1 \mu\text{m}$, the dielectric permittivity of paraelectric STO ceramics increases first and then decreases with an increase in grain

size and reaches a maximum value at $1 \mu\text{m}$. In contrast, in the grain-size range of $1.12\text{--}43.8 \mu\text{m}$, the dielectric permittivity, ferroelectricity, and piezoelectric constant of ferroelectric BTO ceramics all decrease with an increase in grain size, and they exhibit typical grain-size effects. As expected, the variation of the flexoelectric coefficient of STO ceramics with grain size is completely consistent with that of the dielectric permittivity, showing a significant dielectric permittivity dependence. This indicates that the dielectric permittivity dominates the intrinsic flexoelectric grain-size effect in the absence of the ferroelectric factor.

However, for BTO ceramics, the flexoelectric coefficient shows the opposite trend with an increase in grain size, which is positively correlated with the grain size (rather than the dielectric permittivity). These results exclude the main contribution of the dielectric permittivity and residual piezoelectricity to the flexoelectric grain-size effect of ferroelectric BTO ceramics. By observing the domain structure and characterizing the I - E curves of the materials, we conclude that the gradually increasing 180° domains in the large grains, which are more likely to be deflected with an electric field, are the main factor that induces the larger flexoelectricity in BTO ceramics.

Flexoelectricity has shown its application potential in the fields of sensing and actuation [17,82]. A research focus is to design and develop high-performance flexoelectric materials to achieve high-performance sensing and actuating devices. Doping is an effective method to enhance the flexoelectricity of materials, but, at the same time, it will also greatly modify the properties of the materials (such as the Curie temperature), which is not desirable for the enhancement of device performance in specific environments [83]. The reported flexoelectric grain-size effect provides more feasible solutions for improving the performance of flexoelectric sensors and actuators. On the other hand, the use of flexoelectricity to develop an alternative type of random access memory with mechanical stress to complete the “write” operation brings different applications for functional materials [14], but the role of flexoelectricity on the ferroelectric domains is still unclear. The electromechanical behavior of different domain structures under the flexoelectric field reported here will provide further guidance for this role, which is expected to bring about innovations in ferroelectric memory based on flexoelectricity.

Data that support the findings of this study are available from the corresponding author upon reasonable request.

ACKNOWLEDGMENTS

This work is supported by the National Natural Science Foundation of China (Grants No. 51962020, No. 12174174, No. 11604135, and No. 11574126) and the Natural Science Foundation of Jiangxi Province (Grants

No. 20212ACB214011 and No. 20202ZDB01006). L.S. is grateful for support from Nanchang University.

-
- [1] A. Abdollahi, F. Vasquez-Sancho, and G. Catalan, Piezoelectric Mimicry of Flexoelectricity, *Phys. Rev. Lett.* **121**, 205502 (2018).
- [2] X. T. Zhang, Q. Pan, D. X. Tian, W. F. Zhou, P. Chen, H. F. Zhang, and B. J. Chu, Large Flexoelectriclike Response from the Spontaneously Polarized Surfaces in Ferroelectric Ceramics, *Phys. Rev. Lett.* **121**, 057602 (2018).
- [3] L. L. Shu, X. Y. Wei, T. Pang, X. Yao, and C. L. Wang, Symmetry of flexoelectric coefficients in crystalline medium, *J. Appl. Phys.* **110**, 104106 (2011).
- [4] M. Stengel, Surface control of flexoelectricity, *Phys. Rev. B* **90**, 201112 (2014).
- [5] G. Catalan, A. Lubk, A. H. G. Vlooswijk, E. Snoeck, C. Magen, A. Janssens, G. Rispens, G. Rijnders, D. H. A. Blank, and B. Noheda, Flexoelectric rotation of polarization in ferroelectric thin films, *Nat. Mater.* **10**, 963 (2011).
- [6] X. Wen, D. F. Li, K. Tan, Q. Deng, and S. P. Shen, Flexoelectret: An Electret with a Tunable Flexoelectriclike Response, *Phys. Rev. Lett.* **122**, 148001 (2019).
- [7] A. Biancoli, C. M. Fancher, J. L. Jones, and D. Damjanovic, Breaking of macroscopic centric symmetry in paraelectric phases of ferroelectric materials and implications for flexoelectricity, *Nat. Mater.* **14**, 224 (2015).
- [8] L. L. Shu, R. H. Liang, Z. G. Rao, L. F. Fei, S. M. Ke, and Y. Wang, Flexoelectric materials and their related applications: A focused review, *J. Adv. Ceram.* **8**, 153 (2019).
- [9] M. Ravnik and J. C. Everts, Topological-Defect-Induced Surface Charge Heterogeneities in Nematic Electrolytes, *Phys. Rev. Lett.* **125**, 037801 (2020).
- [10] Q. Deng, L. P. Liu, and P. Sharma, Electrets in soft materials: Nonlinearity, size effects, and giant electromechanical coupling, *Phys. Rev. E* **90**, 012603 (2014).
- [11] J. Narvaez, F. Sancho, and G. Catalan, Enhanced flexoelectric-like response in oxide semiconductors, *Nature* **538**, 219 (2016).
- [12] L. L. Shu, S. M. Ke, L. F. Fei, W. B. Huang, Z. G. Wang, J. H. Gong, X. N. Jiang, L. Wang, F. Li, S. J. Lei, *et al.*, Photoflexoelectric effect in halide perovskites, *Nat. Mater.* **19**, 605 (2020).
- [13] H. Lu, C. W. Bark, D. E. Ojos, J. Alcala, C. B. Eom, G. Catalan, and A. Gruverman, Mechanical writing of ferroelectric polarization, *Science* **336**, 59 (2012).
- [14] P. Zubko, G. Catalan, A. Buckley, P. R. L. Welche, and J. F. Scott, Strain-Gradient-Induced Polarization in SrTiO₃ Single Crystals, *Phys. Rev. Lett.* **99**, 167601 (2007).
- [15] Y. L. Xia, Y. Ji, Y. Liu, L. Wu, and Y. Yang, Controllable piezo-flexoelectric effect in ferroelectric Ba_{0.7}Sr_{0.3}TiO₃ materials for harvesting vibration energy, *ACS Appl. Mater. Interfaces* **14**, 36763 (2022).
- [16] B. J. Chu, W. Y. Zhu, N. Li, and L. E. Cross, Flexure mode flexoelectric piezoelectric composites, *J. Appl. Phys.* **106**, 104109 (2009).
- [17] U. K. Bhaskar, N. Banerjee, A. Abdollahi, Z. Wang, D. G. Schlom, G. Rijnders, and G. Catalan, A flexoelectric microelectromechanical system on silicon, *Nat. Nanotechnol.* **11**, 263 (2016).
- [18] B. Wang, H. D. Lu, C. W. Bark, C. B. Eom, A. Gruverman, and L. Q. Chen, Mechanically induced ferroelectric switching in BaTiO₃ thin films, *Acta. Mater.* **193**, 151 (2020).
- [19] T. D. Nguyen, S. Mao, Y. W. Yeh, P. K. Purohit, and M. C. McAlpine, Nanoscale flexoelectricity, *Adv. Mater.* **25**, 946 (2013).
- [20] V. Indenbom, E. Loginov, and M. Osipov, The flexoelectric effect and the structure of crystals, *Sov. Phys. Crystallogr.* **26**, 656 (1981).
- [21] A. K. Tagantsev, Piezoelectricity and flexoelectricity in crystalline dielectrics, *Phys. Rev. B* **34**, 5883 (1986).
- [22] R. Resta, Towards a Bulk Theory of Flexoelectricity, *Phys. Rev. Lett.* **105**, 127601 (2010).
- [23] J. W. Hong and D. Vanderbilt, First-principles theory of frozen-ion flexoelectricity, *Phys. Rev. B* **84**, 4193 (2011).
- [24] M. Stengel, Unified *ab initio* formulation of flexoelectricity and strain-gradient elasticity, *Phys. Rev. B* **93**, 245107 (2016).
- [25] W. H. Ma and L. E. Cross, Flexoelectric polarization of barium strontium titanate in the paraelectric state, *Appl. Phys. Lett.* **81**, 3440 (2002).
- [26] W. H. Ma and L. E. Cross, Observation of the flexoelectric effect in relaxor Pb(Mg_{1/3}Nb_{2/3})O₃ ceramics, *Appl. Phys. Lett.* **78**, 2920 (2001).
- [27] L. L. Shu, T. Li, Z. G. Wang, F. Li, L. F. Fei, Z. G. Rao, M. Ye, S. M. Ke, W. B. Huang, Y. Wang, and X. Yao, Flexoelectric behavior in PIN-PMN-PT single crystals over a wide temperature range, *Appl. Phys. Lett.* **111**, 162901 (2017).
- [28] H. C. Xiang, Y. Bai, J. Varghese, C. C. Li, L. Fang, and H. Jantunen, Ultralow temperature cofired BiZn₂VO₆ dielectric ceramics doped with B₂O₃ and Li₂CO₃ for ULTCC applications, *J. Am. Ceram. Soc.* **102**, 1218 (2019).
- [29] Z. H. Dai, S. X. Guo, Y. Gong, and Z. G. Wang, Semiconductor flexoelectricity in graphite-doped SrTiO₃ ceramics, *Ceram. Int.* **47**, 6535 (2021).
- [30] F. Li, D. B. Lin, Z. B. Chen, Z. X. Cheng, J. L. Wang, C. C. Li, Z. Xu, Q. W. Huang, X. Z. Liao, L. Q. Chen, T. R. Shrout, and S. J. Zhang, Ultrahigh piezoelectricity in ferroelectric ceramics by design, *Nat. Mater.* **17**, 349 (2018).
- [31] F. Li, M. J. Cabral, B. Xu, Z. X. Cheng, E. C. Dickey, J. M. LeBeau, J. L. Wang, J. Luo, S. Taylor, W. Hackenberger, *et al.*, Giant piezoelectricity of Sm-doped Pb(Mg_{1/3}Nb_{2/3})O₃-PbTiO₃ single crystals, *Science* **364**, 264 (2019).
- [32] J. Junquera and P. Ghosez, Critical thickness for ferroelectricity in perovskite ultrathin films, *Nat. Mater.* **422**, 506 (2003).
- [33] D. D. Fong, G. B. Stephenson, S. K. Streiffer, J. A. Eastman, O. Auciello, P. H. Fuoss, and C. Thompson, Ferroelectricity in ultrathin perovskite films, *Science* **304**, 1650 (2004).
- [34] M. T. Buscaglia, M. Viviani, V. Buscaglia, L. Mitoseriu, A. Testino, P. Nanni, Z. Zhao, M. Nygren, C. Harnagea,

- D. Piazza, and C. Galassi, High dielectric constant and frozen macroscopic polarization in dense nanocrystalline BaTiO₃ ceramics, *Phys. Rev. B* **73**, 064114 (2006).
- [35] P. Zheng, J. L. Zhang, Y. Q. Tan, and C. L. Wang, Grain-size effects on dielectric and piezoelectric properties of poled BaTiO₃ ceramics, *Acta Mater.* **60**, 5022 (2012).
- [36] I. Fujii, M. Ugorek, and S. Trolier-McKinstry, Grain size effect on the dielectric nonlinearity of BaTiO₃ ceramics, *J. Appl. Phys.* **107**, 104116 (2010).
- [37] V. Buscaglia, M. T. Buscaglia, M. Viviani, L. Mitoseriu, P. Nanni, V. Trefiletti, P. Piaggio, I. Gregora, T. Ostapchuk, J. Pokorny, and J. Petzelt, Grain size and grain boundary-related effects on the properties of nanocrystalline barium titanate ceramics, *J. Eur. Ceram. Soc.* **26**, 2889 (2006).
- [38] D. Ghosh, A. Sakata, J. Carter, P. A. Thomas, H. Han, J. C. Nino, and J. L. Jones, Domain wall displacement is the origin of superior permittivity and piezoelectricity in BaTiO₃ at intermediate grain sizes, *Adv. Funct. Mater.* **24**, 885 (2014).
- [39] V. R. Mudinepalli, L. Feng, W. C. Lin, and B. S. Murty, Effect of grain size on dielectric and ferroelectric properties of nanostructured Ba_{0.8}Sr_{0.2}TiO₃ ceramics, *J. Adv. Ceram.* **4**, 46 (2015).
- [40] P. Zheng, J. L. Zhang, Y. Tan, and C. L. Wang, Grain-size effects on dielectric and piezoelectric properties of poled BaTiO₃ ceramics, *Acta Mater.* **60**, 5022 (2012).
- [41] Y. Huan, X. H. Wang, J. Fang, and L. T. Li, Grain size effect on piezoelectric and ferroelectric properties of BaTiO₃ ceramics, *J. Eur. Ceram. Soc.* **34**, 1445 (2014).
- [42] W. R. Buessem, L. E. Cross, and A. K. Goswami, Phenomenological theory of high permittivity in fine-grained barium titanate, *J. Am. Ceram. Soc.* **49**, 33 (1966).
- [43] Y. Q. Tan, G. Viola, V. Koval, C. Y. Yu, A. Mahajan, J. L. Zhang, H. B. Zhang, X. S. Zhou, N. V. Tarakina, and H. X. Yan, On the origin of grain size effects in Ba(Ti_{0.96}Sn_{0.04})O₃ perovskite ceramics, *J. Eur. Ceram. Soc.* **39**, 2064 (2019).
- [44] A. J. Bell, A. J. Moulson, and L. E. Cross, The effect of grain-size on the permittivity of BaTiO₃, *Ferroelectrics* **54**, 487 (1984).
- [45] G. Arlt, D. Hennings, and G. de With, Dielectric-properties of fine-grained barium-titanate ceramics, *J. Appl. Phys.* **58**, 1619 (1985).
- [46] See the Supplemental Material at <http://link.aps.org/supplemental/10.1103/PhysRevApplied.18.064017> for (1) SEM for SrTiO₃ ceramics; (2) the elimination of oxygen vacancies for BaTiO₃ ceramics; (3) the temperature dielectric spectrum; and (4) piezoresponse force microscopy for BaTiO₃ ceramics, which includes Refs. [11,47–54].
- [47] W. Guo, Z. Ma, Y. Luo, Y. Chen, Z. Yue, and L. Li, Structure, defects, and microwave dielectric properties of Al-doped and Al/Nd co-doped Ba₄Nd_{9.33}Ti₁₈O₅₄ ceramics, *J. Adv. Ceram.* **11**, 629 (2022).
- [48] X. Zhang, N. Chang, J. Zhang, Y. Zhou, Z. Yue, and L. Li, Low-loss (1-x)Ba_{0.6}Sr_{0.4}La₄Ti₄O_{15-x}CaTiO₃ microwave dielectric ceramics with medium permittivity, *J. Alloys Compd.* **819**, 153011 (2020).
- [49] Y. Zhao, B. Yang, Y. Liu, Y. Zhou, Q. Wu, and S. Zhao, Capturing carriers and driving depolarization by defect engineering for dielectric energy storage, *ACS Appl. Mater. Interfaces* **14**, 6547 (2022).
- [50] H. Ullmann and N. Trofimenko, Estimation of effective ionic radii in highly defective perovskite-type oxides from experimental data, *J. Alloys Compd.* **316**, 153 (2001).
- [51] J. Kim, M. You, K. E. Kim, K. Chu, and C. H. Yang, Artificial creation and separation of a single vortex-antivortex pair in a ferroelectric flatland, *npj Quantum Mater.* **4**, 29 (2019).
- [52] I. K. Bdikin, A. L. Kholkin, A. N. Morozovska, S. V. Svechnikov, S. H. Kim, and S. V. Kalinin, Domain dynamics in piezoresponse force spectroscopy: Quantitative deconvolution and hysteresis loop fine structure, *Appl. Phys. Lett.* **92**, 182909 (2008).
- [53] Z. G. Wang, C. C. Li, Z. Zhang, Y. M. Hu, W. B. Huang, S. M. Ke, R. K. Zhen, F. Li, and L. L. Shu, Interplay of defect dipole and flexoelectricity in linear dielectrics, *Scr. Mater.* **210**, 114427 (2022).
- [54] C. A. Mizzi, B. H. Guo, and L. D. Marks, Twin-boundary-mediated flexoelectricity in LaAlO₃, *Phys. Rev. Mater.* **5**, 064406 (2021).
- [55] V. Brize, G. Gruener, J. Wolfman, K. Fatyeyeva, M. Tabellout, M. Gervais, and F. Gervais, Grain size effects on the dielectric constant of CaCu₃Ti₄O₁₂ ceramics, *Mater. Sci. Eng., B* **129**, 135 (2006).
- [56] T. T. Fang, H. L. Hsieh, and F. S. Shiao, Effects of pore morphology and grain size on the dielectric properties and tetragonal-cubic phase transition of high-purity barium titanate, *J. Am. Ceram. Soc.* **76**, 1205 (1993).
- [57] S. H. Yoon, D. W. Kim, S. Y. Cho, and K. S. Hong, Investigation of the relations between structure and microwave dielectric properties of divalent metal tungstate compounds, *J. Eur. Ceram. Soc.* **26**, 2051 (2006).
- [58] T. L. Phan, P. Zhang, D. Gringting, S. C. Yu, N. X. Nghia, N. V. Dang, and V. D. Lam, Influences of annealing temperature on structural characterization and magnetic properties of Mn-doped BaTiO₃ ceramics, *J. Appl. Phys.* **112**, 013909 (2012).
- [59] Y. I. Kim, J. K. Jung, and K. S. Ryu, Structural study of nano BaTiO₃ powder by Rietveld refinement, *Mater. Res. Bull.* **39**, 1045 (2004).
- [60] S. Zhou, D. B. Lin, Y. M. Su, L. Zhang, and W. G. Liu, Enhanced dielectric, ferroelectric, and optical properties in rare earth elements doped PMN-PT thin films, *J. Adv. Ceram.* **10**, 98 (2021).
- [61] T. Hoshina, Size effect of barium titanate: Fine particles and ceramics, *J. Ceram. Soc. Jpn.* **121**, 156 (2013).
- [62] P. Zubko, G. Catalan, and A. K. Tagantsev, Flexoelectric effect in solids, *Annu. Rev. Mater. Res.* **43**, 387 (2013).
- [63] C. A. Mizzi, B. H. Guo, and L. D. Marks, Experimental determination of flexoelectric coefficients in SrTiO₃, KTaO₃, TiO₂, and YAlO₃ single crystals, *Phys. Rev. Mater.* **6**, 055005 (2022).
- [64] J. W. Hong and D. Vanderbilt, First-principles theory and calculation of flexoelectricity, *Phys. Rev. B* **88**, 174107 (2013).
- [65] W. H. Ma and L. E. Cross, Flexoelectricity of barium titanate, *Appl. Phys. Lett.* **88**, 232902 (2006).
- [66] J. Narvaez, S. Saremi, J. W. Hong, M. Stengel, and G. Catalan, Large Flexoelectric Anisotropy in Paraelectric Barium Titanate, *Phys. Rev. Lett.* **115**, 037601 (2015).
- [67] W. Z. Yao, J. L. Zhang, X. M. Wang, C. M. Zhou, X. Sun, and J. Zhan, High piezoelectric performance and domain

- configurations of $(\text{K}_{0.45}\text{Na}_{0.55})(0.98\text{Li}_{0.02}\text{Nb}_{0.76}\text{Ta}_{0.18}\text{Sb}_{0.06}\text{O}_3$ lead-free ceramics prepared by two-step sintering, *J. Eur. Ceram. Soc.* **39**, 287 (2019).
- [68] G. Arlt and P. Sasko, Domain configuration and equilibrium size of domains in BaTiO_3 ceramics, *J. Appl. Phys.* **51**, 4956 (1980).
- [69] G. Arlt, Twinning in ferroelectric and ferroelastic ceramics: Stress relief, *J. Mater. Sci.* **25**, 2655 (1990).
- [70] J. E. Chou, M. H. Lin, and H. Y. Lu, Ferroelectric domains in pressureless-sintered barium titanate, *Acta Mater.* **48**, 3569 (2000).
- [71] M. Eriksson, H. X. Yan, G. Viola, H. P. Ning, D. Gruner, M. Nygren, M. J. Reece, and Z. J. Shen, Ferroelectric domain structures and electrical properties of fine-grained lead-free sodium potassium niobate ceramics, *J. Am. Ceram. Soc.* **94**, 3391 (2011).
- [72] Y. Q. Tan, J. L. Zhang, C. L. Wang, G. Viola, and H. X. Yan, Enhancement of electric field-induced strain in BaTiO_3 ceramics through grain size optimization, *Phys. Status Solidi A* **212**, 433 (2014).
- [73] G. Ark, The influence of microstructure on the properties of ferroelectric ceramics, *Ferroelectrics* **104**, 217 (1990).
- [74] H. T. Martirena and J. C. Burfoot, Grain-size effects on properties of some ferroelectric ceramics, *J. Phys. C: Solid State Phys.* **7**, 3182 (1974).
- [75] D. Berlincourt and H. A. Krueger, Domain processes in lead titanate zirconate and barium titanate ceramics, *J. Appl. Phys.* **30**, 1804 (1959).
- [76] E. C. Subbara, M. C. McQuarrie, and W. R. Buessem, Domain effects in polycrystalline barium titanate, *J. Appl. Phys.* **28**, 1194 (1957).
- [77] H. X. Yan, F. Inam, G. Viola, H. P. Ning, H. T. Zhang, Q. H. Jiang, T. Zeng, Z. P. Gao, and M. J. Reece, The contribution of electrical conductivity, dielectric permittivity and domain switching in ferroelectric hysteresis loops, *J. Adv. Dielectr.* **1**, 107 (2011).
- [78] K. Wang and J. F. Li, $(\text{K}, \text{Na})\text{NbO}_3$ -based lead-free piezoceramics: Phase transition, sintering and property enhancement, *J. Adv. Ceram.* **1**, 24 (2012).
- [79] J. Narvaez and G. Catalan, Origin of the enhanced flexoelectricity of relaxor ferroelectrics, *Appl. Phys. Lett.* **104**, 162903 (2014).
- [80] G. Arlt, D. Hennings, and G. Dewith, Dielectric properties of fine-grained barium titanate ceramics, *J. Appl. Phys.* **58**, 1619 (1985).
- [81] Y. L. Qin, J. L. Zhang, W. Z. Yao, C. L. Wang, and S. J. Zhang, Domain structure of potassium-sodium niobate ceramics before and after poling, *J. Am. Ceram. Soc.* **98**, 1027 (2015).
- [82] Q. Deng, S. H. Lv, Z. Q. Li, K. Tan, X. Liang, and S. P. Shen, The impact of flexoelectricity on materials, devices, and physics, *J. Appl. Phys.* **128**, 080902 (2020).
- [83] C. C. Li, Z. G. Wang, F. Li, Z. G. Rao, W. B. Huang, Z. J. Shen, S. M. Ke, and L. L. Shu, Large flexoelectric response in PMN-PT ceramics through composition design, *Appl. Phys. Lett.* **115**, 142901 (2019).